Latin American Journal of Solids and Structures
www.lajss.org

Stress concentration around perforations produced by corrosion in steel storage tanks

Abstract

This paper presents numerical results of stress concentration factors for plates perforated by corrosion. Evidence from 25 plates with corrosion perforation considered show that typical shapes may be characterized as a deviation from an ellipse or from a circle. In order to model typical perforations created by this type of corrosion, holes with non-circular boundaries have been considered in the form of cosine shape and variations from it. Two load cases are investigated: uniaxial and shear stress fields in an elastic plane stress problem. The influence of the amplitude of deviation with respect to an ellipse or circle and the local curvature of the internal boundary of the hole are studied. A simplified model of an equivalent ellipse originally proposed by Nishida is shown to provide good estimates for stress concentration factors for a range of shapes induced by corrosion.

Keywords

finite element analysis, oil tanks, corrosion, steel tanks, stress concentration factors.

Luis A. Godoy[a*]
Adrián D. Boccardo[b]
Francisco J. Rodríguez[b]
Patricia M. Dardati[b]

[a] Structures Department, FCEFyN, Universidad Nacional de Córdoba, and CONICET, Córdoba 5000, Argentina

[b] Mechanical Engineering Department and CIII, Facultad Regional Córdoba, UTN, Córdoba, Argentina

* Corresponding Author Email: lgodoy@efn.uncor.edu

1 INTRODUCTION

Pitting corrosion is a frequent form of damage found in crude oil, diesel, and fuel oil steel storage tanks (Yamaguchi *et al.* 2006). This is a localized form of corrosion with very small dimensions with respect to the overall dimensions of the plate which is exposed to a corrosive agent. As a consequence of pitting corrosion, a cavity with irregular boundaries may form in the metal or it may lead to full perforation of the plate. It has been shown that such local effects may have significant consequences on the behavior of thin walled structures (Godoy 1996).

Although most tank components are exposed to environmental agents, the bottom plate and the lower part of the cylindrical container are affected at a higher rate than other parts of the tank because water accumulates at the bottom and below the fuel content. Such water contains chlorides and sediments, which are responsible for the high corrosion rate. Pitting corrosion of lower parts in

tanks tends to be hidden in a tank filled with fuel, and is only visible during inspections of an empty tank. Further, sediments that deposit in pitting holes make it more difficult to identify the problem during inspections. This form of corrosion is shown in Figure 1 for the bottom plate of a steel storage tank. The photographs show both sides of the plate, and it may be seen that corrosion starts at the internal surface. The actual contours of the perforations are not a circular or elliptical hole, but they have an irregular shape which is characterized by lobes that depart from the circular shape. Only a few papers have been concerned with efs of corrosion on tanks (Maheri and Abdollahi 2013).



(a)



(b)

Figure 1: Corrosion perforations in a steel plate at the bottom of a tank, showing (a) external and (b) internal surfaces (Photographs by Dr. M. Salazar).

According to Myers, "pitting corrosion in structural members is not serious provided that the strength is not reduced substantially" (Myers, 1997, pp. 99). What constitutes a substantial reduction is not clear unless structural evaluation is performed, and this has been done by several researchers who considered various failure mechanisms. First, the influence of pitting corrosion on the buckling of in-plane loaded flat plates has been investigated as a cause of reduction of buckling loads. In the context of stability of ship hull plates and stiffened panels, the influence of pitting

corrosion has been addressed by Guedes Soares and coworkers (see, for example, Jiang and Guedes-Soares 2012, Silva *et al.* 2013). Along this line, Mahammad *et al.* (2010) investigated plates with corrosion on both surfaces, for stiffened as well as unstiffened plates. Mahammad *et al.* (2012) considered plate buckling and post-buckling behavior and proposed a simplified effective thickness methodology to account for pit corrosion affecting one side of a plate. For steel tubes, local corrosion effects on strength and buckling was studied in Nazari *et al.* (2014). Paik *et al.* (2004) studied ultimate strength of plates with pit corrosion.

A second problem investigated in the literature is the stress concentration around pitting corrosion in plates; in which pitting is frequently modeled as a cavity which does not penetrate the plate thickness. Two dimensional studies of a hemispherical pit under in-plane uniaxial stresses were pioneered by Eubanks (1954), followed by Fujita *et al.* (1978), and Pidaparti and Patel (2008), among others. Three dimensional analysis of a semielliptical corrosion pit has been reported by Cerit *et al.* (2009) for various pit depths and diameters; these authors found that the stress concentration is dominated by the ratio between major and minor axis of the ellipse and proposed a simple approximate expression to estimate Stress Concentration Factors.

This paper is concerned with corrosion effects that penetrate through the plate thickness and the stress concentrations induced under in-plane loads, both uniaxial and shear loads. The investigation is conducted numerically using finite element analysis. Two shapes of the contour of the perforation caused by corrosion are explored in this paper, together with the influence of the main parameters involved. Analytical approximations are also considered to estimate stress concentration factors, and their limits of validity are assessed.

2 TYPICAL GEOMETRIES AND STRESS CONCENTRATIONS IN CORROSION PERFORATIONS

2.1 Geometry of corrosion perforations

Geometries of typical corrosion perforations have been here studied based on evidence from perforated plates such as that shown in Figure 1. Twenty five perforations from samples of steel plates obtained from tanks with corrosion were considered in this research in order to identify geometric ranges of representative perforations.

An ellipse was initially taken as a basic shape to represent the perforation and deviations from the elliptical shape to fit actual contours of perforations were measured from photographs. Fitting an ellipse into an irregular shape was done using a minimum square algorithm.

The results of this limited number of observations are presented in Figure 2(a), in which the aspect ratio of the ellipse (in terms of the relation between major and minor diameters of the ellipse, a/b) has been plotted as a function of the number of waves n that approximate the contour. The maximum deviation with respect to the ellipse, d, versus the number of waves n that approximate the contour, has been plotted in Figure 2(b).

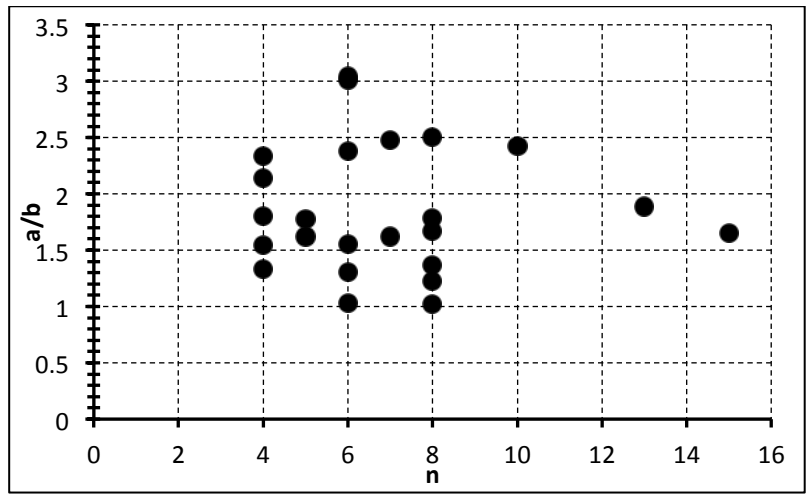

(a)

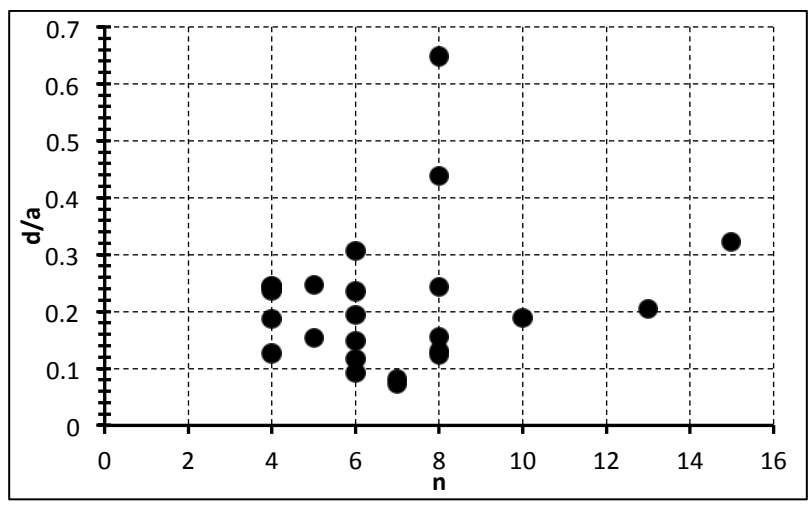

(b)

Figure 2: Geometric parameters for corrosion perforations. (a) Relation between ellipse axis a/b for various number of waves n; (b) Normalized deviation of contour from an ellipse, a/R, for various number of waves n.

The results of Figure 2 are only illustrative of shapes induced by corrosion, but they provide an expected range of geometric parameters which may be found in typical situations. Regarding the shape of the ellipse that may approximate the perforation, the observations indicate that relations a/b range between 1 (which is a circular hole) and 4. Typical deviations from that elliptical shape were found to be between d/a = 0.05 and 0.5, where a is the major diameter of the ellipse. The number of waves around the contour of the perforation was found to be between n = 4 and n = 15, where n is the number of full waves. Of course, perforations in other examples could be found to be outside these ranges, but those given here seem to be a reasonable starting point to investigate stress concentrations around non-elliptical holes.

2.2 Stress distributions around a perforation

To illustrate the stress redistribution in the vicinity of a corrosion perforation, the actual geometries of two holes have been investigated. The chosen geometries have contours that exhibit different features: one with a rather symmetric contour, and a second hole with an asymmetric shape. The effects due to corrosion have been modeled in two-dimensional plates under in-plane loading with a perforation in the form of a hole with non-circular boundaries. The geometries of the two real holes have been modeled using the general purpose finite element software ABAQUS (2006). The computations were performed using an eight-node quadrangular element designated as CPS8.

In the first case studied, the real contour shown in Figure 3 was investigated. Under uniaxial loads, the results show stress concentrations at some points with Sc = 12.6. Shear load was also considered for the same geometry, leading to Sc = 14.9.

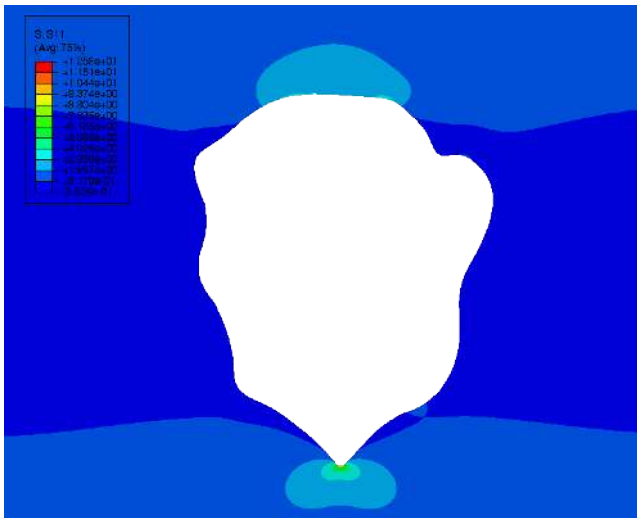

(a)

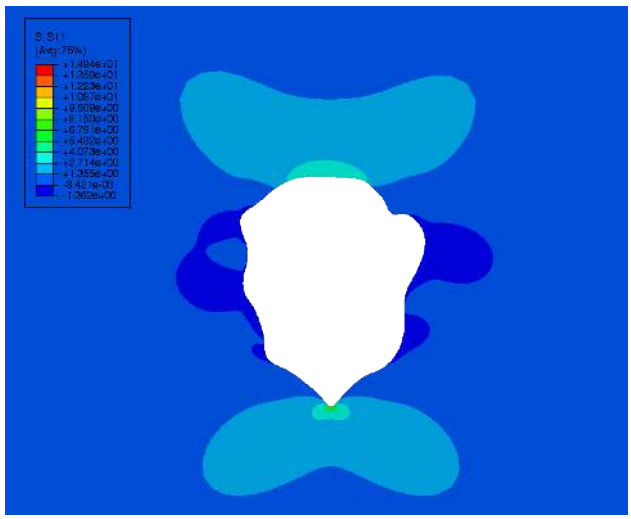

(b)

Figure 3: Case Study 1 of real corrosion perforation. (a) Uniaxial load; (b) Shear load.

The second case investigated has the asymmetric shape shown in Figure 4. Results of the real geometry under uniaxial load are illustrated in Figure 4(a), with stresses characterized by Sc = 8.45. For the same geometry, shear loading induced a Stress Concentration Factor Sc = 10.08.

In both perforations investigated, the stress redistribution concentrates the highest values of stresses in zones of high curvature of the contour, without showing interaction between two adjacent lobes. This indicates that values of Sc are dominated by local details of the geometry rather than global differences in the complete contour of the perforation.

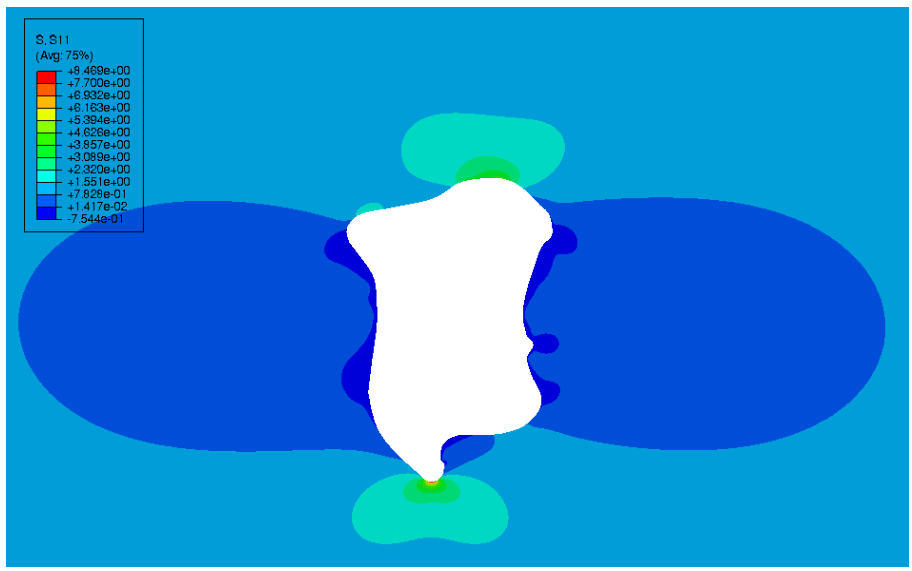

(a)

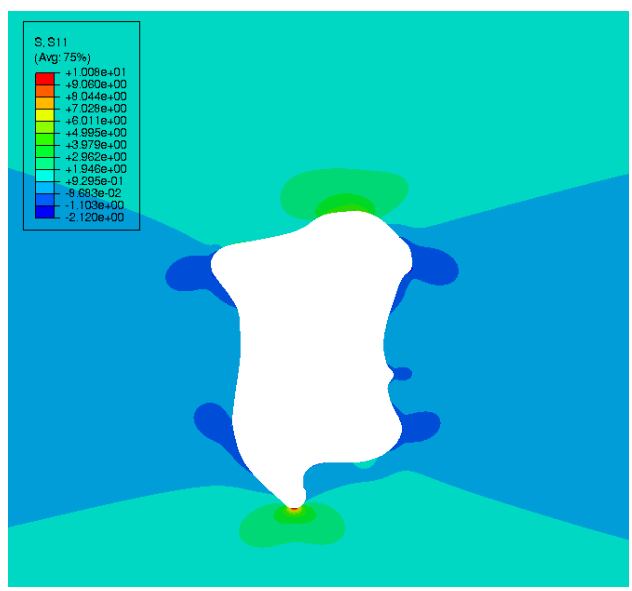

(b)

Figure 4: Case Study 2 of real corrosion perforation. (a) Uniaxial load; (b) Shear load.

These two cases were chosen because they have different contours and show that values of Sc could be in the order of 12 under uniaxial stress field, whereas values of Sc = 15 could be expected for shear load.

2.3 Simplified estimates using an equivalent ellipse

Approximations to estimate stress concentration factors in shallow grooves have been proposed in the literature, in which the actual groove is substituted by an equivalent ellipse having the same depth and minimum radius of curvature of the grove (Pilkey and Pilkey, 2008, pp. 19). The concept of an equivalent ellipse was originally used by Nishida (1976) to account for an hexagonal hole under a uniaxial stress field, i.e. a hole with an irregular contour having six "grooves" (or waves, as they are called in this paper) around a circumference. Although the hole has six waves, an ellipse is fitted to two of them facing each other. According to Nishida, the difference in Stress Concentration Factor between the actual hexagonal hole and the equivalent ellipse is of less than 10%.

The analytical equation of Stress Concentration Factors Scu for uniaxial and Scs shear load are respectively (Pilkey and Pilkey, 2008):

$$\mathrm{Scu} = 1 + 2\sqrt{\frac{1}{\mathrm{Rc}}} \tag{1}$$

$$\mathrm{Scs} = 2\left(1 + \sqrt{\frac{1}{\mathrm{Rc}}} + \sqrt{\mathrm{Rc}}\right) \tag{2}$$

where Rc is the radius of curvature of the boundary at the crest with maximum curvature.

The above equations have been used to represent the two cases studied in the previous section, but addressing only the zone of high curvature as extremes of an equivalent ellipse. Thus, case 1 in Figure 3 can be idealized using ellipse parameters a/b = 5.52. The resulting concentration factor becomes Scu = 12.04 under uniaxial load and Scs = 13.4 under shear.

For the second case studied Figure 4, an idealization by means of an ellipse leads to an ellipse with a/b = 3.55. Values of Scu = 8.1 and Scs = 9.67 are computed for this case. Comparison of the approximate solutions given by eqn. (1) and (2) with those of the finite element discretization show differences in the order of 6%, which is considered as a good estimate

But rather than investigating actual shapes associated with specific examples, it is worth considering more regular geometries defined with respect to circular and elliptical perforations; this is the subject of the next section.

3 STRESSES AROUND PERIODIC NON-CIRCULAR PERFORATIONS

To illustrate the effect of the shape of the inner boundary of the perforation, two cases are considered in the following: a cosine boundary and a star-like boundary.

3.1 Perforation in the form of a cosine boundary

A cosine shape of the boundary has been assumed by superposing a cosine curve to a circular hole, as shown in Figure 5(a), so that the radius r of the boundary is defined as:

$$r = R + d \cdot \cos(n \cdot \theta) \tag{3}$$

where R is the circular hole radius, d is the amplitude of the cosine curve (deviation with respect to the circular hole); and n is the number of full waves, as shown in Figure 5(a). The influence of the boundary is investigated by changing the amplitude d and the number of waves n.

The radius of curvature of the boundary at the crest is given by

$$Rc = \frac{[r^2 + (r')^2]^{3/2}}{2 \cdot (r')^2 - r \cdot r'' + r^2} \tag{4}$$

This radius Rc can be written in terms of d and n by substitution of eqn. (3) into eqn. (4) and evaluating at $\vartheta = 0$, leading to:

$$Rc|_{\theta=0} = \frac{1}{d \cdot n^2 + \dfrac{1}{1+d}} \tag{5}$$

Due to symmetry of the problem in terms of geometry and loading, only one-quarter of the plate was discretized, as shown in Figure 5(b). The computations were performed using the general purpose finite element program ABAQUS with eight-node quadrangular elements CPS8. Based on convergence studies, a finite element mesh with 60,000 elements was adopted, as shown in Figure 6.

Values of d/R between 0.025 and 0.3 were considered in the computations for n between 4 and 32, to investigate the influence of d and n on the Stress Concentration Factor.

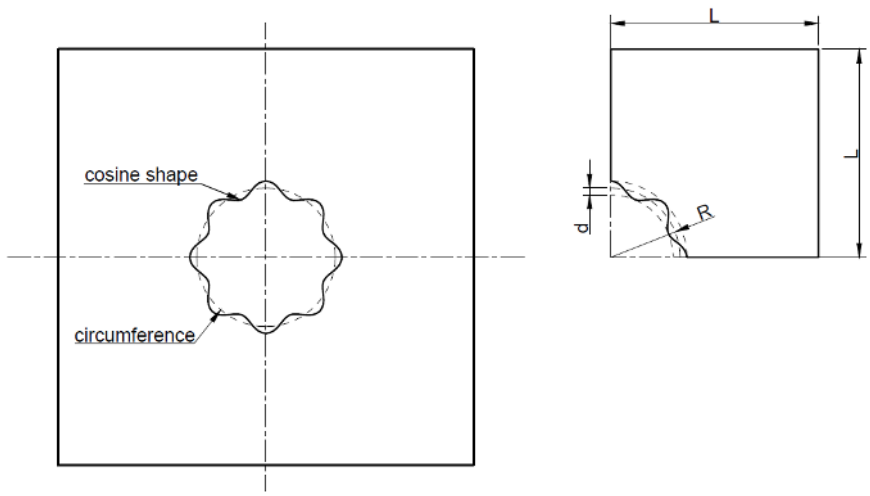

(a) (b)

Figure 5: Hole with an irregular boundary defined by a cosine curve superposed on a circular hole, with n = 8. (a) Domain considered. (b) Definition of geometric parameters.

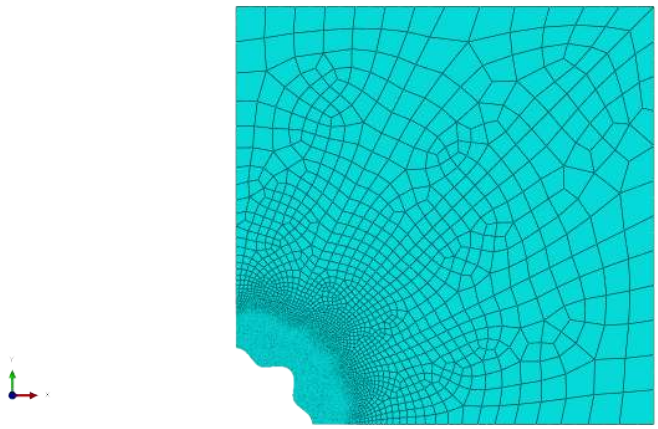

Figure 6: Mesh generated for a plate with pit with cosine boundary with n = 8, using plane stress elements CPS8.

3.2 Perforation with a star-like boundary

A slightly different form of boundary has also been investigated in order to assess the effects of the boundary shape on the Stress Concentration Factor. The hole perforated by corrosion has a star-like shape in this case, with a smoothed curve at the tips of the star in order to avoid singularities which would be more typical of cracks. The assumed star is shown in Figure 7. The shape of the star is defined to have the same radius of curvature at the tips as in the cosine geometry described in the previous section. This allows having a different shape with straight sides, for which the minimum curvature is the same as in the cosine shape. A comparison of the two geometries is illustrated in Figure 8.

Again, quadratic quadrilaterals elements (identified a CPS8 in ABAQUS) were used to carry out the computations, using the same ranges of d/R and n as in the cosine boundary.

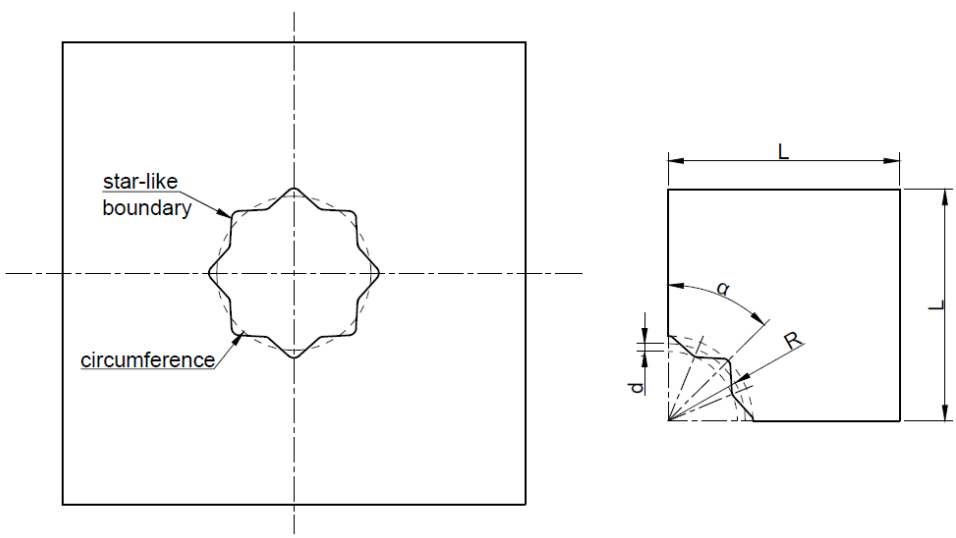

(a) (b)

Figure 7: A star-like hole with n = 8. (a) Domain considered. (b) Definition of geometric parameters.

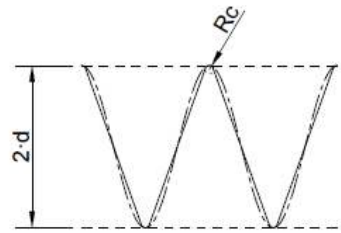

Figure 8: Comparison of the two idealized contours considered in this paper.

4 RESULTS FOR PERIODIC NON-CIRCULAR PERFORATIONS

The results of Stress Concentration Factors Sc for various geometries of boundaries of a perforation identified by d/R = 0.025, 0.05, 0.1, and 0.3, and for n= 4, 8, 16, and 32, are presented in Table 1 (for uniaxial load) and in Table 2 (for shear load) for the two models discussed in Section 3 and the equivalent ellipse approximation described in Section 2.3. The data has been plotted in terms of angle $\alpha = 2\pi/n$, and is shown in Figures 9 to 14.

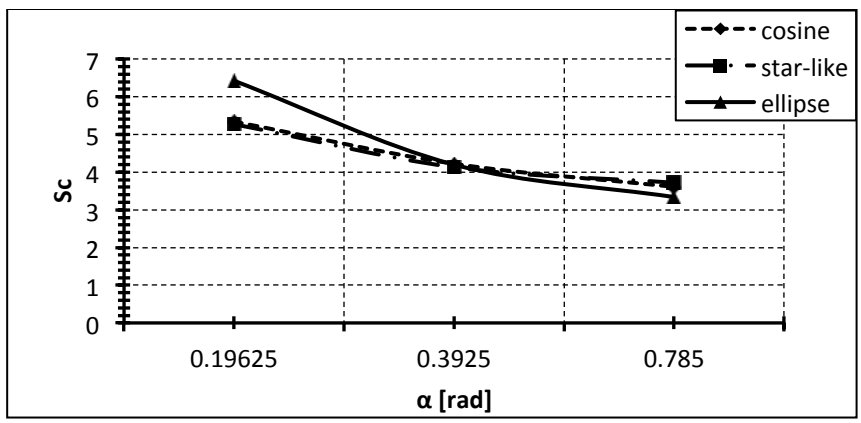

Figure 9: Stresses in a plate with d/R = 0.025 under uniaxial load.

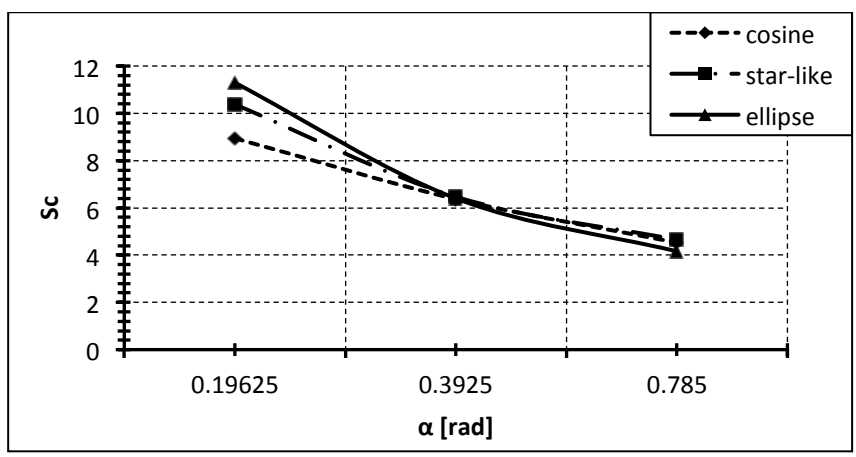

Figure 10: Stresses in a plate with d/R = 0.1 under uniaxial load.

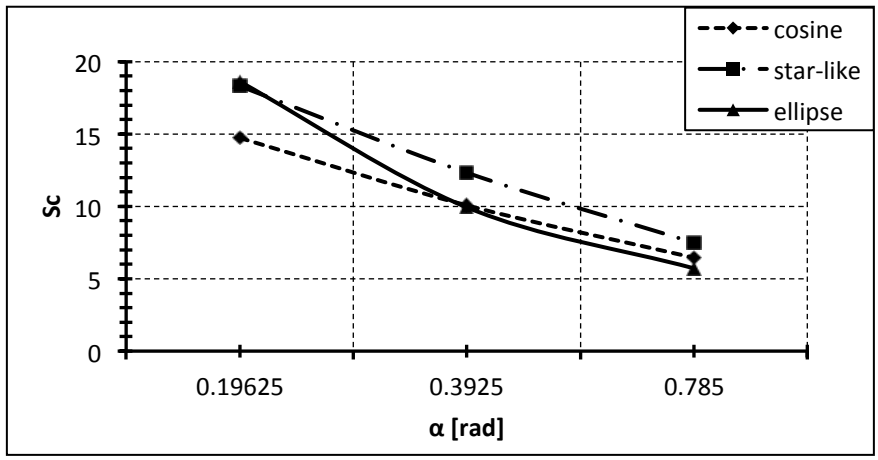

Figure 11: Stresses in a plate with d/R = 0.3 under uniaxial load.

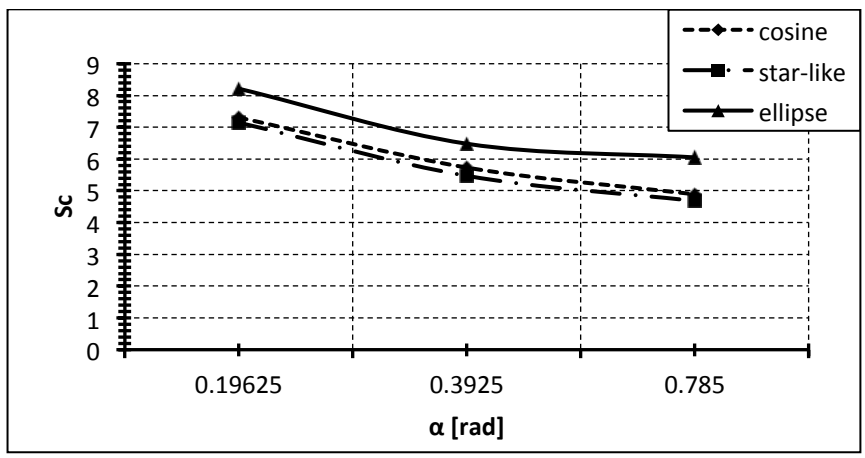

Figure 12: Stresses in a plate with d/R = 0.025 under shear load.

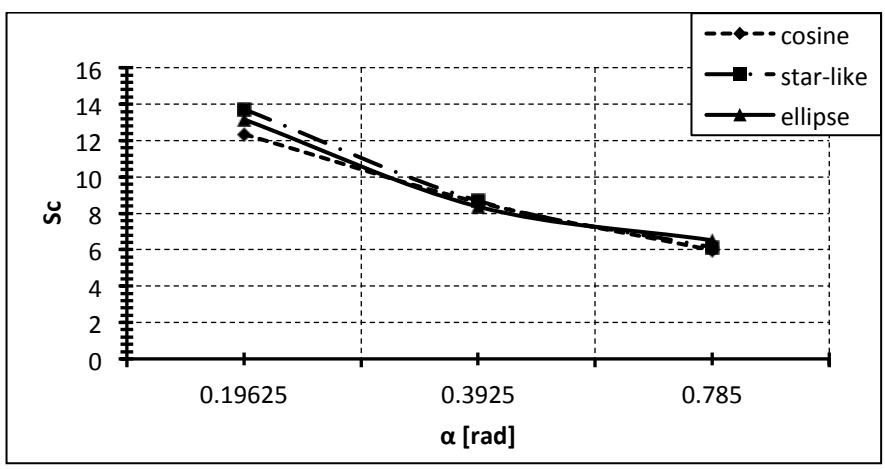

Figure 13: Stresses in a plate with d/R = 0.1 under shear load.

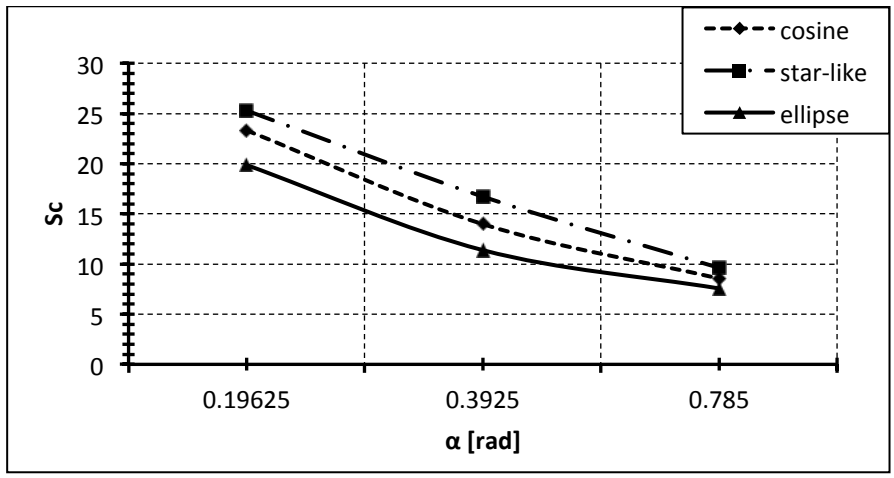

Figure 14: Stresses in a plate with d/R = 0.3 under shear load.

4.1 Effect of contour waviness

The influence of the waviness of the contour in the model has been investigated by considering changes in the number of waves n. The number of waves is associated with the value of the minimum radius of curvature, so that it is expected that higher values of Sc should be obtained with increasing values of n.

This influence may be observed in the results of Table 1 for uniaxial load in the cosine contour of a hole; for example, for a given amplitude d/R = 0.1, Sc increases from 4.5 (for n = 4) to 6.3 (for n = 8) and to 8.9 (for n = 16). This is also shown in Figures 9, 10 and 11 in terms of the circumferential angle α, thus indicating an almost linear relation between Sc and α for large values of α, with nonlinearity being noticeable for small α. A similar trend occurs in the results for shear load shown in Figures 12, 13 and 14.

4.2 Effect of contour shape

For a small amplitude of penetration with respect to the circular hole, say d/R = 0.025, similar results are obtained under uniaxial load between the cosine and star-like models (see Figures 9 and 12). But for a higher value of d, say d/R = 0.1, the results of the star-like model tend to deviate from those of the cosine model, thus predicting higher Stress Concentration Factors. In terms of central angle α, this effect is more evident for small angles but it is not noticeable for large angles. In summary, for large central angles, it is not possible to distinguish between models of cosine and star boundaries, but the differences become important if the angle becomes small.

The simplified model, in which an ellipse is assumed to fit the minimum curvature of the contour, leads to very good values for large central angles of the boundary, but it overestimates Sc for both uniaxial and shear loading for small α. Only for the case of d/R = 0.1 the simplified ellipse model approaches the star-like shape.

4.3 Effect of wave amplitude

The influence of the amplitude d of penetration of corrosion with respect to a circular hole has been investigated next. The increase of d is associated with the value of the minimum radius of curvature, so that it is expected to have higher values of Sc with increasing d. This is shown in the results of Tables 1 and 2, and may be identified by comparison of Figures 9 and 11 (for uniaxial load) and 12 and 14 (for shear load).

	d/R											
	0.3			0.1			0.05			0.025		
n	cosine	star-like	ellipse	cosine	star-like	ellipse	cosine	star-like	ellipse	cosine	star-like	ellipse
4	6.45	7.49	5.72	4.53	4.65	4.16	3.95	3.86	3.64	3.62	3.72	3.34
8	10.07	12.33	9.93	6.37	6.47	6.40	5.07	5.00	5.07	4.22	4.13	4.20
16	14.73	18.33	18.61	8.96	10.38	11.29	6.86	7.03	8.41	5.35	5.28	6.43

Table 1: Values of Stress Concentration Factors Sc in a plate under uniaxial load.

	d/R											
	0.3			0.1			0.05			0.025		
n	cosine	star-like	ellipse	cosine	star-like	ellipse	cosine	star-like	ellipse	cosine	star-like	ellipse
4	8.55	9.62	7.56	5.97	6.13	6.52	5.27	5.15	6.18	4.88	4.68	6.05
8	13.97	16.72	11.38	8.56	8.69	8.37	6.82	6.54	7.13	5.71	5.47	6.48
16	23.31	25.31	19.84	12.20	13.72	13.17	9.32	9.54	10.12	7.26	7.15	8.22

Table 2: Values of Stress Concentration Factors Sc in a plate under shear load.

For example, assuming a cosine boundary of the corroded zone, and for n = 8, an increase in amplitude from d/R = 0.025 to 0.05 leads to an increase in Sc of almost 20% (from 5.71 to 6.82), whereas an increase of 50% (to Sc = 8.56) is obtained in going from d/R = 0.025 to d/R = 0.1. This is a nonlinear effect in terms of the amplitude, and may also be verified to occur for the star boundary described in Section 2.2.

4.4 Effect of interaction between waves

As the number of waves increases (or else, the central angle in the contour decreases), there is a redistribution in the stress field due to interaction between neighboring parts on the contour. This is shown in Figure 15 for a star-like contour, in which the stress redistribution for two cases are shown for d/R = 0.1, one with n = 8 and a second one with n = 16.

For the case with n = 8, the values of maximum stresses are of 6.5 for a unit value of the stress field at a distance in horizontal direction of the figure. As the number n increases to 16, the value of maximum stress increases to 10. This significant increase is due to an increase in the local curvature, but it is also accompanied by an interaction between waves along the contour. An isolated ellipse, on the other hand, would produce even higher values of stresses, leading to an 11% increase with respect to the case with n = 16. This indicates that there is a shielding effect due to the close

proximity of waves along the contour, and explains why the simplified model of an ellipse fails to predict accurate values as the number n increases.

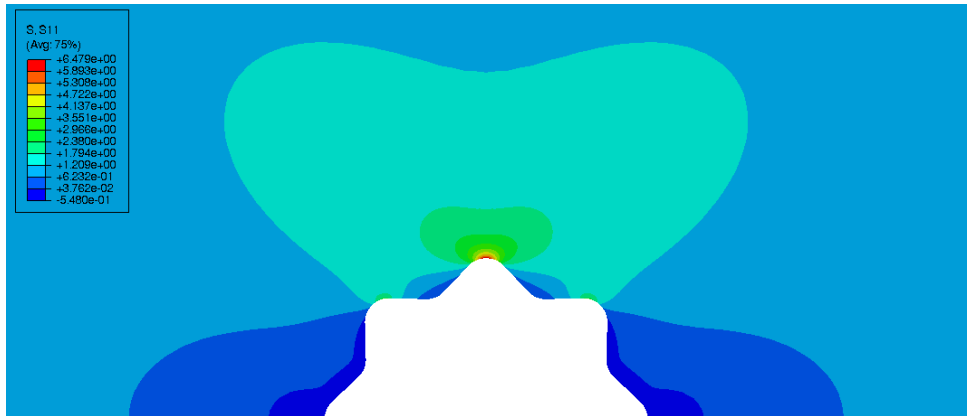

(a)



(b)

Figure 15: Effect of stress interaction between along the contour under uniaxial load in the horizontal direction (x1). Stresses in x1 direction, S11, in a plate with (a) d/R = 0.1 and n= 8. (b) d/R = 0.1 and n= 16.

5. CONCLUSIONS

Estimates of stress concentration factors have been made in this research for plates having perforations similar to those due to corrosion. The models discussed in this paper assume a non-circular boundary, having cosine or star-like shapes, with the number of waves and the depth of the penetration with respect to a circular hole as variables. Such periodic geometries are idealizations with respect to real situations, which are characterized by more irregular shapes, such as those shown in Figure 1. However, they illustrate the influence of various geometric parameters and allow comparisons with even more simplified models of an ellipse.

Several conclusions may be drawn from the study:

(a) The geometries of real corrosion perforations have been characterized with reference to an ellipse as a basic shape and deviations from it in the form of an amplitude d and a number of waves n. For a limited number of samples (25 corrosion perforations), the diameters of the basic ellipse ranged between $1 < a/b < 4$, with $4 < n < 15$. For the same set of samples, the amplitude had deviations d with respect to the ellipse of $0.05 < d/a < 0.5$.

(b) Values of stress concentration factors under shear are approximately 30 to 35% higher than those obtained under a uniaxial stress field.
(c) Based on the results of Figures 9 to 14, stress concentration factors of up to 20 are expected in plates with perforations due to pit corrosion. This is a substantial increase with respect to a circular hole, which is associated to a factor of 3. The concentration factors increase with the amplitude, as reflected by the ratio d/R in this work.
(d) The actual shape of the contour has an influence for small central angle of the waves along the contour, but is not a major issue for large central angles.
(e) For large central angles of the waves, an ellipse leads to good estimates of Stress Concentration Factors, but it has large errors for small angles. The simplified model of an ellipse does not yield upper or lower bounds for Stress Concentration Factors in this problem and the estimates depend on the ratio d/R and angle α.

Acknowledgements

The authors thank Dr. Mónica Salazar (National University of Comahue, Argentina) for providing the photographs of Figure 1. The results of this paper are part of a project on the behavior of steel storage tanks, supported by grants of SECYT-UNC and CONICET (PIP 112-201201-00126-CO). L Godoy is a member of the research staff of CONICET (Investigador Superior). A Boccardo and F Rodriguez had a doctoral scholarship from CONICET during this research.

References

ABAQUS (2006). Documentation, version 6.6, Hibbitt, Karlsson and Sorensen, Providence, RI.

Cerit, M., Genel, K., Eksi, S. (2009). Numerical investigation on stress concentration of corrosion pit, Engineering Failure Analysis, 16: 2467-2472

Eubanks, R.A. (1954). Stress concentration due to a hemispherical pit at a free surface, J. Applied Mechanics, 21(3): 57-62.

Fujita, T., Sadayasu, T., Tsuchida, E., Nakahara, I. (1978). Stress concentration due to a hemispherical pit at a free surface of a thick plate under all-around tension, Bulletin of the JSME, 21: 561-565.

Godoy, L.A. (1996). Thin-walled Structures with Structural Imperfections, Pergamon Press, Oxford.

Jiang, X., Guedes-Soares, C. (2012). A closed form formula to predict the ultimate capacity of pitted mild steel plate under biaxial compression, Thin-Walled Structures, 59: 27–34.

Mahammad, Z.H., Nouri, E., Khedmati, M.R., Roshanali, M.M. (2010). Degradation of the compressive strength of unstiffened/stiffened steel plates due to both sides randomly distributed corrosion wastage, Latin American Journal of Solids and Structures, 7: 335-367.

Mahammad, Z.H., Nouri, E., Khedmati, M.R., Sadeghifard, S. (2012). An effective thickness proposal for strength evaluation of one-side pitted steel plates under uniaxial compression, Latin American Journal of Solids and Structures, 9: 475-496.

Maheri, M.R., Abdollahi, A. (2013). The effects of longer uniform corrosion on the buckling of ground based steel tanks under seismic loading, Thin-Walled Structures, 62: 1-9.

Myers, P.E. (1997). Aboveground Storage Tanks, McGraw Hill, New York.

Nazari, M., Khedmati, M.R., Khalaj, A.F. (2014). A numerical investigation into ultimate strength and buckling behavior of locally corroded steel tubular members, Latin American Journal of Solids and Structures, 11: 1063-1076.

Nishida, M. (1976). Stress Concentration, Mori Kita Press, Tokyo (in Japanese).

Paik, J.K., Lee, J.M., Ko, M.J. (2004). Ultimate shear strength of plate elements with pit corrosion wastage, Thin-Walled Structures, 42: 1161–1176.

Pidaparti, R.M., Patel, R.R. 2008. Correlation between corrosion pits and stresses in Al alloys, Material Letters, 62: 4497-4499.

Pilkey, W.D., Pilkey, D.F. (2008). Peterson's Stress Concentration Factors, Third Ed., Wiley.

Silva, J.E., Garbatov, Y., Guedes-Soares, C. (2013). Ultimate strength assessment of rectangular steel plates subjected to random localized corrosion degradation. Engineering Structures, 52: 295-305.

Yamaguchi, S., Ishida, K., Ibata, T., Kawano, K., Sekine, K., Maruyama, H. (2006). A study of influence of locally reduced thickness on stress of bottom annular plate of oil storage tank during uplifting by seismic loading. In: Proceedings of the ASME PVP Conference on Maintenance and Safe Operation, Vancouver, Canada, 23–27.